
CG-FedLLM: HOW TO COMPRESS GRADIENTS IN FEDERATED FUNE-TUNING FOR LARGE LANGUAGE MODELS

A PREPRINT

Huiwen Wu
Zhejiang Laboratory
Hangzhou, Zhejiang, China
huiwen0820@outlook.com

Xiaohan Li
Zhejiang Laboratory
Hangzhou, Zhejiang, China
xiaohan@zhejianglab.com

Deyi Zhang
Zhejiang Laboratory
Hangzhou, Zhejiang, China
xiaohan@zhejianglab.com

Xiaogang Xu *
Huawei Technology Inc.
Hangzhou, Zhejiang, China
xiaogangxu00@gmail.com

Jiafei Wu †
Zhejiang Laboratory
Hangzhou, Zhejiang, China
wujiafei@zhejianglab.com

Puning Zhao
Zhejiang Laboratory
Hangzhou, Zhejiang, China
pnzhao@zhejianglab.com

Zhe Liu
Zhejiang Laboratory
Hangzhou, Zhejiang, China
zhe.liu@zhejianglab.com

May 24, 2024

ABSTRACT

The success of current Large-Language Models (LLMs) hinges on extensive training data that is collected and stored centrally, called Centralized Learning (CL). However, such a collection manner poses a privacy threat, and one potential solution is Federated Learning (FL), which transfers gradients, not raw data, among clients. Unlike traditional networks, FL for LLMs incurs significant communication costs due to their tremendous parameters. In this study, we introduce an innovative approach to compress gradients to improve communication efficiency during LLM FL, formulating the new FL pipeline named **CG-FedLLM**. This approach integrates an encoder on the client side to acquire the compressed gradient features and a decoder on the server side to reconstruct the gradients. We also develop a novel training strategy that comprises Temporal-ensemble Gradient-Aware Pre-training (**TGAP**) to identify characteristic gradients of the target model and Federated AutoEncoder-Involved Fine-tuning (**FAF**) to compress gradients adaptively. Extensive experiments confirm that our approach reduces communication costs and improves performance (e.g., average **3** points increment compared with traditional CL- and FL-based fine-tuning with **LlaMA** on a well-recognized benchmark, C-Eval). This is because our encoder-decoder, trained via **TGAP** and **FAF**, can filter gradients while selectively preserving critical features. Furthermore, we present a series of experimental analyses that focus on the signal-to-noise ratio, compression rate, and robustness within this privacy-centric framework, providing insight into the development of more efficient and secure LLMs.

1 Introduction

Recently, a soaring development of Large Language Models (LLMs) has emerged since the introduction of ChatGPT [27], exploring its strong capabilities in mathematics reasoning [20], natural language understanding [22], and

*corresponding author

†corresponding author

common sense reasoning [34, 45]. Despite the advanced capabilities of general LLMs, their practical application remains challenging due to issues in training strategies and data management. For the **training strategy**, fine-tuning is essential to adapt general LLMs to specific practical fields before application. However, due to the large number of parameters in LLMs, managing the entire parameter set on a standard, low-cost GPU, such as the RTX 4090, is impractical, even for models like LLaMA-7B [38]. Therefore, an efficient fine-tuning technique, such as LoRA [18], is used to selectively adjust a subset of parameters. Regarding **training data**, fine-tuning LLMs necessitates substantial amounts of high-quality data. However, stringent data privacy laws such as the General Data Protection Regulation (GDPR) [43] and the California Consumer Privacy Act (CCPA) [7] significantly limit data sharing across platforms. Federated learning (FL) offers a promising solution to privacy concerns and has already achieved significant success with traditional neural networks [28, 24]. **Therefore, there is an immediate need to establish a federated strategy to efficiently fine-tune LLM, named FedLLM.**

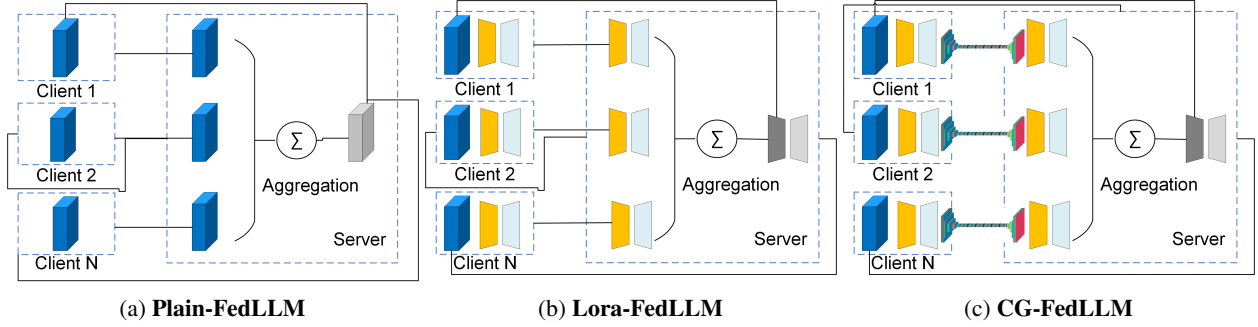


Figure 1: Design Variants of FL Approaches for LLMs

In FL, clients perform local stochastic gradient descent on their datasets and transmit gradients or incremental model updates to a central server, as shown in Fig.1a. This server aggregates these local gradients and redistributes the averaged gradients back to the clients, thus incurring communication costs between local and global entities in FL. The communication costs of applying FL to LLMs could be prohibitive due to the contradiction between limited bandwidth and extensive parameters. Even if we employ LoRA to fine-tune partial layers (as displayed in Fig.1b), for example, 8B parameters for typical LoRA-based fine-tuning **LLaMA-7B** [38]. Consequently, enhancing communication efficiency requires further compression. However, typical strategies such as predefined quantization pipelines inevitably lead to information loss. Thus, selecting an appropriate compression technique is crucial to ensure both a satisfied compression ratio and minimal distortion in transmitted gradients.

In this paper, we develop a novel learnable gradient compression method to implement a FedLLM satisfied, which is called **CG-FedLLM**. In **CG-FedLLM**, an AutoEncoder is used where clients compress their gradients into compact features using the encoder **E**, and the server reconstructs these features into accurate gradients with the decoder **D**, as illustrated in Fig. 1c. The primary challenge lies in training **E** and **D** to accurately reconstruct the gradient without compromising privacy. To address this, we divide the training process into two stages, named Gradient-aware Pre-training (**TGAP**) and Federated AutoEncoder-involved Fine-tuning (**FAF**).

To ensure compression accuracy, a direct approach is to train the AutoEncoder alongside the LLM. However, this method incurs substantial additional training costs. Furthermore, the *dynamic* nature of the training samples, due to the varying gradients of the target model during training, complicates the fitting process. Therefore, we identify the characteristics of the target model’s gradients and design a time-ensemble pre-training scheme to train **E** and **D**, called **TGAP**. Observations indicate that, while the gradient values change over the course of training, their distributions remain similar. Therefore, by recording the gradients of the target model in various training stages, we can create a *consistent and homogeneous* data set \mathcal{A} to effectively train our AutoEncoder. This data set can be compiled through the cooperation of various clients prior to FL, by aggregating their local gradients. Empirical evidence suggests that by pretraining **E** and **D** with such a gradient data set before FL, the AutoEncoder can efficiently reconstruct gradients during FL without the need for further training. **TGAP** has not violated the privacy premise, since no raw data is shared to formulate \mathcal{V} and the AutoEncoder can be placed in a Trusted Execution Environment (TEE) [6, 3] to train (only needs a few minutes).

After securing the necessary AutoEncoder via **TGAP**, it can be integrated into a new federated fine-tuning pipeline (outlined in Algorithm 1), termed **FAF**. Compared to traditional federated fine-tuning, this method only requires additional execution of the **E** and **D** forwards, which is minimal in cost as **E** and **D** can be designed to be lightweight with simple structures.

In addition to communication efficiency, extensive experiments on established LLM benchmarks demonstrate that fine-tuning LLMs with our **CG-FedLLM** achieves superior performance compared to traditional FL and centralized learning (CL). This is attributed to the trained AutoEncoder’s ability not only to accurately reconstruct useful gradients for training, but also to correct abnormal gradients with distinct distributions, a capability derived from the inherent nature of deep neural networks to adjust aberrant signals [41]. Furthermore, our **CG-FedLLM** is effectively compatible with differential privacy mechanisms, enhancing privacy protection. It has been empirically demonstrated that noise added to the gradient can be filtered out by the encoder and cleanly reconstructed by the decoder.

The main contributions of our work are threefold:

- We have developed a new federated fine-tuning framework, CG-FedLLM, which incorporates an AutoEncoder into FL to significantly enhance communication efficiency.
- To ensure the AutoEncoder performs well without incurring additional training costs in FAF, we designed TGAP to pre-train the AutoEncoder prior to implementing FL.
- Extensive evaluations, including the multilevel C-Eval benchmark, affirm that the model fine-tuned with CG-FedLLM has better performance compared with traditional FL and CL.

2 Related Work

Parameter-Efficient Fine-Tuning (PEFT). PEFT methods tackle the challenges of memory and computational demands when adapting extensive language models for specific applications [13, 25, 9]. Popular techniques in PEFT involve adjusting LLM parameters within a low-rank confined subspace, such as LoRA (low-rank adaptation) [18], which achieves considerable resource savings while preserving efficacy. PEFT [17] mitigates elevated communication expenses by fine-tuning a minor segment of the overall parameters in conventional NLP tasks. DoRA [26] divides the initial model weights into magnitude and direction to facilitate fine-tuning, employing LoRA to alter the aspect of direction. QLoRA [8] shows that fully precision adapters can be efficiently trained on lower precision models while ensuring sustained performance. REFT [50] functions on an unaltered base model and acquires task-specific modifications in hidden representations. Although these methods significantly reduce parameter updates, communication costs remain considerable in federated learning scenarios for LLMs with many clients and limited network bandwidth.

Federated learning. Federated Learning (FL) is a general training scheme to collaboratively train a deep learning models without sharing the raw data [30, 51, 24]. In the FL settings, the client train its own model with a local dataset and send the increment gradients to the server, and the server aggregates the partial gradients and synchronizes with the local clients. In this procedure, there are two important issues that influence the practical adoption of the FL model, which are the communication bottleneck [4, 23, 35] and privacy guarantee [31, 39, 2]. Existing methods to alleviate communication cost in traditional FL include low-bit quantization [32, 33] and sparsification [44, 48]. However, these methods may lead to performance degradation due to information distortion. Moreover, research attempts to learn a gradient compression model with CNN networks of 1 dimension which does not scale to LLM due to the huge size of model parameters [1]. Existing methods to ensure privacy in FL including differential privacy [49, 40], secret sharing [29, 2], and homomorphic encryption [12, 53]. However, differential privacy causes the degradation of FL training due to the added random noise. Secret sharing exerts an additional cost of communication while homomorphic encryption increases the computation complexity trendingly due to the encryption and decryption procedures. Thus, these methods cannot fully address the privacy issue in federated LLM training in a practical way.

3 Methodology

In Sect.3.1, we provide an overview of our CG-FedLLM and highlight its differences from traditional FL. Sect.3.2 details the implementation of the AutoEncoder used in CG-FedLLM and analyzes its communication benefits in Sect.3.3. Sect.3.4 summarizes the FL algorithm in CG-FedLLM, utilizing our trained AutoEncoder. Finally, in Sect. 3.5, we discuss the privacy advantages of our approach and its compatibility with other privacy-enhancing techniques, such as differential privacy.

3.1 Overview

Given a target LLM M , there are N clients and a global server S in FL. In FL’s setting, each client i will have its own training dataset \mathcal{D}_i and a copy of model M_i , and training M_i with \mathcal{D}_i can result in a set of gradients to update the model, as G_i . Gradients $G_{i=1,\dots,N}$ will be propagated on the server side S for the ensemble, as $\tilde{G}_{i=1,\dots,N} = T_i(G_{i=1,\dots,N})$, where T_i is the transmission process for the i -th client. $\tilde{G}_{i=1,\dots,N}$ can be combined to produce the polymerized

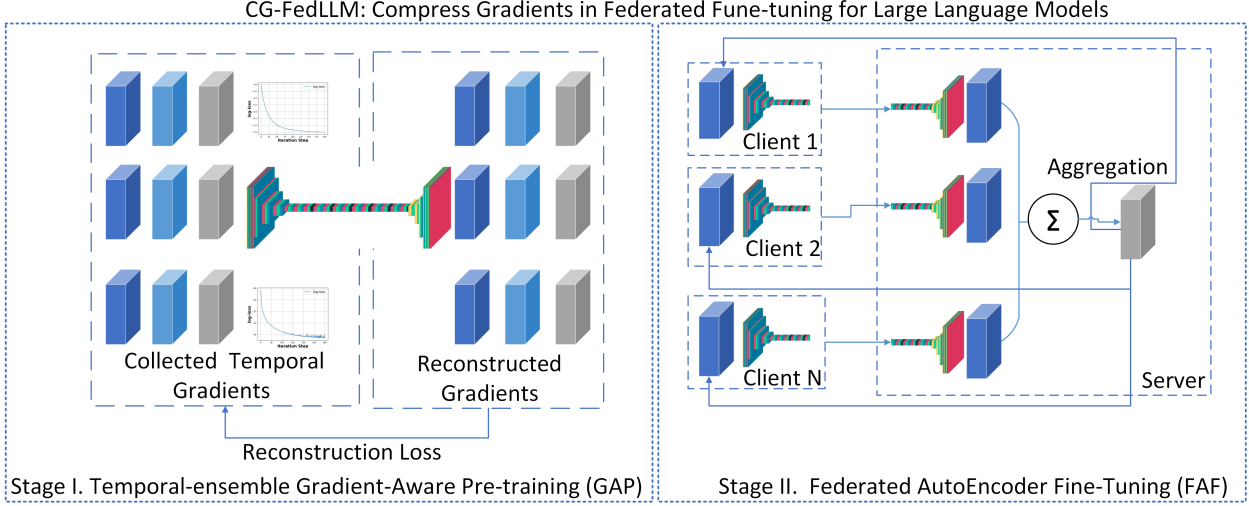


Figure 2: **CG-FedLLM**: Compress Gradients in Federated Fine-tuning for Large Language Models. The AutoEncoder \mathcal{V} involved in **CG-FedLLM** is completed by TGAP (left), and the illustration of utilizing \mathcal{V} in FL is implemented by FAF (right)

gradient \mathbf{G} to update the central model weight, as $\Delta \mathbf{W}_{\text{global}}$. In addition, the global update can be delivered to the selected clients I_t in the iteration step t , updating the weight of each client with $\Delta \mathbf{W}_i$. This is a cyclic process until the training is completed. In traditional FL, $\Delta \mathbf{W}$ and $\Delta \mathbf{W}_{i=1, \dots, N}$ are small in size, resulting in a low communication cost in $\mathbf{T}_{i=1, \dots, N}$. However, this burden becomes overwhelming when applying FL to LLMs due to the vast number of parameters requiring fine-tuning. Even with techniques like LoRA, the transmission of numerous transformer layers remains a challenge for typical LLMs.

In our **CG-FedLLM**, we integrate an adaptive compression model \mathcal{V} into the FL with the AutoEncoder structure, consisting of the encoder **Enc** and the decoder **Dec**. To transmit $\mathbf{G}_{i=1, \dots, N}$ (the gradient can also be first compressed by other methods like Low rank decomposition in LoRA), it will be first transferred into a feature with a tiny size, as

$$\mathbf{F}_{i=1, \dots, N} = \text{Enc}(\mathbf{G}_{i=1, \dots, N}). \quad (1)$$

The server side can receive these features efficiently, and decode them into the desired gradients as

$$\tilde{\mathbf{G}}_{i=1, \dots, N} = \text{Dec}(\mathbf{F}_{i=1, \dots, N}). \quad (2)$$

It should be note that **Enc** and **Dec** are shared among different clients to save the training and memory cost. The differences between **CG-FedLLM** and traditional FL can be seen in Fig. 2.

Training of \mathcal{V} is completed by our designed Temporal-ensemble Gradient-Aware Pre-training (**TGAP**) before FL, and FL with \mathcal{V} is implemented via our designed Federated AutoEncoder Fine-Tuning (**FAF**) algorithm, which will be described in the next two sections.

3.2 Stage I. Temporal-ensemble Gradient-Aware Pre-training (TGAP)

The structure and training of AutoEncoder. The AutoEncoder, comprising **Enc** and **Dec**, processes 2D features and can incorporate various structures, e.g., ResNet [37] and Transformer [42]. The encoder compresses the initial input into a compact latent representation, while the decoder uses this representation to reconstruct the original input, as shown in Eqs. 1 and 2. Our main goal is to explore how to train satisfied E and D , without restrictions on network types. An example is shown in Fig. 3. The training of \mathcal{V} is completed by measuring the error between inputs and outputs, as

$$\mathcal{L}_{\text{recons}} = \|\mathbf{G} - \tilde{\mathbf{G}}\|_2. \quad (3)$$

The difficulty in training the AutoEncoder. To ensure compression accuracy, a straightforward approach is to simultaneously train the AutoEncoder \mathcal{V} with the LLM. However, this strategy incurs significant additional training costs. Additionally, the AutoEncoder’s training set is *dynamic*, as the gradients of the target model continuously evolve during the training process. This variability complicates fitting, as newly acquired knowledge can disrupt previously established patterns. Empirical evidence also indicates that existing continuous learning approaches can lead to failures.

Table 1: Communication Efficiency with Various AutoEncoder Architectures.

	1-D CNN [1]	ResNet [15]	U-Former [47]
G and $\tilde{\mathbf{G}}$	[128, 1, 32768]	[1, 4096, 2048]	[8, 1024, 1024]
Enc(G)	[128, 4, 256]	[64, 64, 32]	[1, 256, 512]
Compressed Ratio	3.21 %	1.56 %	1.56 %

Our strategy for training the AutoEncoder. To avoid the dynamic training of the AutoEncoder, we utilize a pre-training strategy. For each selected client \mathcal{I}_i in the t -th iteration of pre-training, we train the model \mathbf{M}_i with its own training data \mathcal{D}_i without FL. During the training procedure, we can collect the gradient sequences as $\mathbf{G}_{i,t}, i = \{1, \dots, N\}, t = \{1, \dots, T\}$. The distributions of the gradients from varying time steps are also similar, resulting in the homogeneous property for the set of $\mathbf{G}_{i,t}, i = \{1, \dots, N\}, t = \{1, \dots, T\}$. Training \mathcal{V} with $\mathbf{G}_{i,t}, i = \{1, \dots, N\}, t = \{1, \dots, T\}$ avoids the sub-optimization issues caused by dynamic training data while effectively capturing the characteristics of the target model’s gradients across various datasets and training states. It is empirically validated that \mathcal{V} with such pre-training before FL, can have satisfied reconstruction ability during FL.

3.3 The Communication Analysis

During the fine-tuning phase of the LLaMa-7B foundational model, even after employing low-rank decomposition, the challenge of transmitting large model parameters persists. For instance, with a chosen rank number of 8, the parameters to be transmitted in federated fine-tuning is totally $4096 \times 8 \times 2 \times 4 \times 32 = 8,388,608$. When the number of clients N is large, computational efficiency is limited by communication bandwidth. In the second phase of our proposed approach (**CG-FedLLM**), we utilize the AutoEncoder developed in Stage I (**TGAP**) to decrease the communication burden during federated fine-tuning, as only the encoder’s features **Enc(G)** need to be propagated.

Our compression strategy offers advantages over previous methods that use neural networks to reduce communication costs, such as the 1D CNN described in [1]. As detailed in Table 1, we analyze the compression ratio by comparing the parameter sizes before encoding, after encoding, and after decoding across three different AutoEncoders. Crucially, the consistency between the encoder’s input shape and the decoder’s output shape ensures accurate reconstruction of the model parameter increment ΔW . The compression ratio is calculated based on the proportion of total parameters in the encoder’s output relative to its input. A lower compression ratio signifies improved communication efficiency in federated settings. Through a detailed analysis, we found that AutoEncoders using ResNet and U-Former both achieve a compression ratio of 1.56%, compared to the 3.21% achieved by the 1-D CNN. This demonstrates that the 2-D architectures, ResNet and U-Former, are more effective in reducing communication overhead during federated fine-tuning.

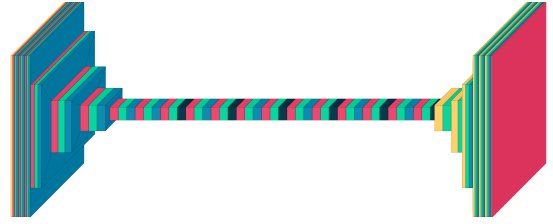


Figure 3: One example for the AutoEncoder’s structure: architecture of compressed CNN visualized by Visual-Keras.

3.4 Stage II. Federated AutoEncoder Fine-Tuning (FAF)

This section outlines the federated fine-tuning pipeline involving \mathcal{V} . Initially, the global model is set up as the foundational model already specified. During iteration t , following the sampling strategy, the server selects a subset of clients I_t according to the sampling ratio α and distributes the global model $\mathbf{W}_{\text{global}}^t$ to these clients. Subsequently, we split the process into two phases. The initial phase occurs on the client side, where each selected client conducts LoRA training locally and updates the local model parameters in a low-rank format, specifically $\Delta \mathbf{W}_i^t = \mathbf{B}_i \mathbf{A}_i, i \in I_t$. Following this, each client compresses the low-rank matrices using a pre-trained encoder, $[\tilde{\mathbf{A}}_i, \tilde{\mathbf{B}}_i] = \text{Enc}[\mathbf{A}_i, \mathbf{B}_i]$, to minimize the uplink communication overhead. These compressed local gradients $[\tilde{\mathbf{A}}_i, \tilde{\mathbf{B}}_i]$ are then transmitted to the server. On the server side, it gathers the compressed data $[\tilde{\mathbf{A}}_i, \tilde{\mathbf{B}}_i]$ sent by the clients. The server processes these matrices independently using the pre-trained decoder to revert them to their original forms, denoted as $[\tilde{\tilde{\mathbf{A}}}_i, \tilde{\tilde{\mathbf{B}}}_i] = \text{Dec}[\tilde{\mathbf{A}}_i, \tilde{\mathbf{B}}_i]$. Post-decompression, an aggregation of the local matrices within the LORA subspace is performed, represented as $[\tilde{\mathbf{A}}, \tilde{\mathbf{B}}] = [\sum_i \tilde{\tilde{\mathbf{A}}}_i, \sum_i \tilde{\tilde{\mathbf{B}}}_i]$. Ultimately, the global model parameters are refreshed using these decompressed and aggregated low-rank matrices $[\tilde{\mathbf{A}}, \tilde{\mathbf{B}}]$. The updated global model will then send the update of the model to the clients,

Algorithm 1 Stage II. Federated AutoEncoder Fine-tuning (FAF)

Input: number of all clients N , local partitioned clients ratio α , foundational model \mathbf{W}_{base} , step size η , pre-trained encoder Enc , pre-trained decoder Dec , number of communication rounds T ;

Output: federated fine-tuned model \mathbf{W}^T ;

Initialize with foundational model: $\mathbf{W}_{\text{global}}^0 = \mathbf{W}_{\text{base}}$ for all $i \in [1, 2, \dots, N]$

for $t := 0$ to $T - 1$ **do**

Server samples a client subset I_t with sampling ratio α

Server sends $\mathbf{W}_{\text{global}}^t$ to all selected clients

Local Training:

for each chosen client $i \in I_t$ **do**

Each client perform LoRA training locally and obtain $\Delta \mathbf{W}_i^t = \mathbf{B}_i \mathbf{A}_i$;

Each client performs the gradient compression with the pre-trained encoder

$$[\bar{\mathbf{A}}_i, \bar{\mathbf{B}}_i] = \text{Enc}[\mathbf{A}_i, \mathbf{B}_i];$$

Each client sends the compressed local gradients $[\bar{\mathbf{A}}_i, \bar{\mathbf{B}}_i]$ to the server;

end for

Server Aggregation:

Server collects the local compressed low rank gradients $[\bar{\mathbf{A}}_i, \bar{\mathbf{B}}_i]$;

Server decompresses local compressed gradients

$$[\tilde{\mathbf{A}}_i, \tilde{\mathbf{B}}_i] = \text{Dec}[\bar{\mathbf{A}}_i, \bar{\mathbf{B}}_i];$$

Server aggregates in the LoRA subspace

$$[\tilde{\mathbf{A}}, \tilde{\mathbf{B}}] = [\sum_i \tilde{\mathbf{A}}_i, \sum_i \tilde{\mathbf{B}}_i];$$

Server updates the global model

$$\mathbf{W}_{\text{global}}^{t+1} = \mathbf{W}_{\text{global}}^t + \Delta \mathbf{W}_i^t = \mathbf{W}_{\text{global}}^t + \tilde{\mathbf{B}} \tilde{\mathbf{A}}.$$

end for

and this procedure between the clients and the server will be cyclic until the end of the training. The overall procedure is summarized in Algorithm. 1.

3.5 Advantage of CG-FedLLM for Further Privacy Protection

Beyond communication efficiency, our CG-FedLLM also offers enhanced privacy protection. Even within FL contexts, studies [56, 14] have shown that the original fine-tuning data can potentially be reconstructed from local gradients shared during federated aggregation. Applying differential privacy to local gradients is a common strategy for ensuring privacy in federated fine-tuning. However, achieving robust privacy protection through differential privacy involves adding significant noise to the transmitted gradients, which can lead to a notable decrease in performance during fine-tuning.

Conversely, our **CG-FedLLM** integrates more effectively with differential privacy due to its robustness against noise added to the gradients. This capability is empirically confirmed in our experiments (Sect. 4.5) and is theoretically attributed to the AutoEncoder’s ability to correct abnormal inputs back to the normal distribution established during training.

4 Evaluation Results

In this section, we evaluate the performance of LLM trained with our CG-FedLLM (**Compress-FT**) against the base model without fine-tuning (**Base**), models trained with traditional FL using LoRA (**LoRA-FT**), and models trained with CL (**Cent**). The implementations for federated fine-tuning in LLMs are based on FedIT [55, 54]. Initially, we provide a overview of the experimental setup, including the selection of foundational models and the federated setting (dataset and division for each client). Then we present detailed evaluation results using C-eval benchmarks [19].

4.1 Foundation Models

We test our methods with various LLM foundation models and mainly adopted the 7B size due to the limitation of the computational resource.

LlaMa-7B [38]. LlaMa consists of a series of foundational language models ranging from 7B to 65B parameters. These models are trained on trillions of tokens from publicly available datasets. The scaled-down LlaMa-13B surpasses GPT-3

(175B) on benchmarks such as MMLU [16]. The LLaMa-7B variant, with 6.7B parameters, includes 32 transformer layers, each containing 32 heads.

Alpaca-7B [36]. The Alpaca-7B model, developed by the Stanford team, is an enhanced version of the LLaMA-7B model, refined using 52,000 instruction-following demonstrations.

ChatGLM-6B [10, 52]. ChatGLM-6B is an open-source, bilingual conversational language model based on the General Language Model framework [11], comprising 6.2 billion parameters.

4.2 Federated Settings

Databricks-dolly-15k [5]. The **Databricks-dolly-15k** dataset is comprised of eight different categories: brainstorming, classification, closed QA, creative writing, general QA, information extraction, open QA and summarization. The data set is divided into 100 segments using the commonly employed category Dirichlet allocation technique [46].

C-eval-dev [19]. The **C-eval-dev** set is utilized for federated fine-tuning purposes. Each “dev” set for a subject includes five exemplars accompanied by explanations for few-shot evaluation. There are 260 training samples in total.

LLaMa-7B and **Alpaca-7B** each have 100 clients with a selection probability of 0.05. **ChatGLM-6B** has 3 clients, each with a selection probability of 1.

4.3 Performance Comparison on C-Eval

C-Eval [19] is a comprehensive Chinese evaluation system designed to assess the advanced knowledge and reasoning skills of foundational models within a Chinese context. It includes 13,948 multiple choice questions across 52 distinct fields, covering various educational stages such as middle school, high school, college, and professional levels. For our evaluation, we use six conventional subject categories: Stem, social sciences, humanities, other, average, and Avg (hard). “Avg (hard)” represents the mean score of the C-Eval HARD benchmark, which covers subjects like advanced mathematics, discrete mathematics, probability and statistics, college chemistry, college physics, high school mathematics, high school chemistry, and high school physics, all requiring significant reasoning skills for resolution.

We present the performance summary with C-Eval in Table 2. We observe that for all base models, our methods (**Compress-FT**) significantly improve performance. For the initial model LLaMa-7B, our approach (**Compress-FT**) enhances the **Base** score from 21.6 to 26.6 in the STEM field, from 23.9 to 25.5 in Humanities, from 23.3 to 25.7 in Other fields, from 22.8 to 26.2 on average, and from 20.3 to 26.8 for the hard level (Avg(Hard)). The performance of the **Compress-FT** approach is comparable to **LoRA-FT**, showing an improvement in total scores in all fields from STEM to Avg (hard), except in the field of Social Sciences. In Social Sciences, **LoRA-FT** records a high score of 27.6, the highest among the methods compared. Interestingly, the **Compress-FT** technique also shows improvements over the centralized fine-tuning methods (**Cent**). This suggests that the fine-tuning methods might be more resilient to minor disturbances caused by the compression process. We observe similar performance improvements when changing the base model to **Alpaca**. The performance of **Compress-FT** with foundational models **LLaMa-7B** and **Alpaca-7B** is on par with **Chinese-LLaMa-13B** and **Chinese-Alpaca-13B** in C-Eval assessments, and it significantly outperforms **ChatGLM-6B**, demonstrating the effectiveness of our approaches. Further details on experiments involving C-Eval can be found.

4.4 The Analysis of Regression via AutoEncoder

The feasibility to compress: the visualization of gradients to propagate. In this section, we show the experimental analysis of compressed data. As mentioned in Sects. 3.3 and 3.4, we compress the gradients processed with LoRA, as **A** and **B**. Using **LLaMa-7B** model, the shapes of the matrices **A**[⊤] and **B** are 8×4096 . We concatenate the matrices **A**[⊤] and **B** for the projection matrices **Q**, **K**, **V**, **O** for 32 Transformers blocks in the first dimension. Thus, the input shape of the AutoEncoder becomes $(8 \times 2 \times 4 \times 32) \times 4096 = 2048 \times 4096$. Figure 4 illustrates the distribution of maximum and minimum values in all concatenated matrices **A** and **B** during TGAP. During training, the maximum values (left) vary from 0.0018 to 0.0010, while the minimum values (right) are symmetrically distributed from -0.0018 to -0.0010. Furthermore, from iterations 1 to 20, there is a noticeable convergence trend in both the maximum and minimum values of the transmitted parameters. Ultimately, the maximum and minimum values of **A** and **B** converge to the order of 10^{-3} , indicating an overall distribution of **A** and **B** approaching zero as iterations increase. This zero gradient value signifies convergence, and the regular evolution of **A** and **B** allows the success of training the AutoEncoder in TGAP.

The convergence analysis of compression networks. In this section, we demonstrate the convergence behavior of TGAP training. In Figure 5, it is evident that compared to the 1D AutoEncoder, the 2D AutoEncoder equipped with CNN and U-former blocks achieves a significantly lower endpoint in the training process, effectively capturing the

Table 2: A Comparison of C-Eval

Methods	Stem	Social Sciences	Humanities	Others	Average	Avg(hard)
Cent-LLaMa	24.5	25.6	25.5	24.4	24.9	23.4
Compress-FT-LLaMa (ours)	26.6	26.5	25.5	25.7	26.2	26.8
LoRA-FT-LLaMa	25.9	27.6	25.2	24.5	25.8	24.8
Base-LLaMa	21.6	23.4	23.9	23.3	22.8	20.3
Cent-Alpaca	25.9	24.8	27.3	24.5	25.7	25.7
Compress-FT-Alpaca (ours)	27.5	25.1	27.1	26.8	26.8	28
LoRA-FT-Alpaca	25.5	27.1	25.3	25.8	25.8	24.2
Base-Alpaca	25.5	27.1	25.4	25.9	25.9	24.1
Cent-ChatGLM-6B	47.4	63	50.7	47.3	51.1	35
Compress-FT-ChatGLM (ours)	47.5	63.5	51	47.7	51.3	34.1
LoRA-FT-ChatGLM	47.4	63.5	50.8	47.7	51.3	34.8
Base-ChatGLM	47.1	63.4	51	47.6	51.1	33.9
Cent-LLaMa-CEval	25.6	26.3	27.3	25.2	26.0	25.7
Compress-FT-LLaMa-CEval (ours)	26.8	25.3	26.4	26.6	26.4	27.2
LoRA-FT-LLaMa-CEval	24.4	24.8	26.5	25.4	25.1	25.0
Base-LLaMa-CEval	21.6	23.4	23.9	23.3	22.8	20.3

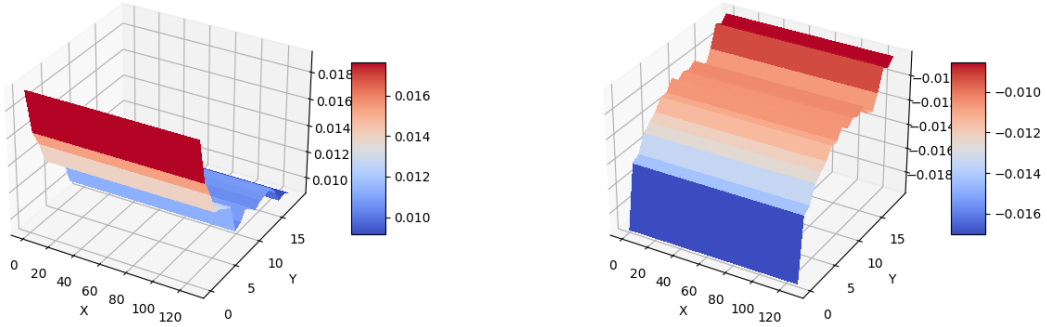


Figure 4: Distribution of maximum values (left) and minimum values (right) of matrices \mathbf{A} 's and \mathbf{B} 's from the iteration 1 to iteration 20. Y axis represents the training epoch, X axis denotes the index of the matrices \mathbf{A} and \mathbf{B} to compress ($2 \times 4 \times 32 = 128$ dimension).

essential information of transmitted gradients. Moreover, among the architectures that incorporate the U-former, the configuration with zero U-former blocks exhibits the highest accuracy in fitting the transmitted data. The smaller log-loss achieved by AutoEncoders contributes to better model performances in C-Eval. We demonstrate this in Sect. 4.5.

Signal Noise Ratio of reconstructed gradients. By analyzing the distribution of the transmitted gradient values described in Figure4 and the MSE loss detailed in Figure5, we can compute the signal-to-noise ratio (SNR) of the reconstructed gradients, which can assess the effects of noise reduction. SNR is characterized as the proportion of signal power relative to noise power [21]. The power of the ℓ_2 norm for the low-rank decomposition of input gradients before compression is displayed in the first row of Table 3. The power of MSE loss calculated between the precompression input data and the post-decompression output data is shown in the second row of Table 3. A higher SNR indicates better preservation of information during the compression process. According to Table 3, the compressor developed using ResNet records the highest SNR, whereas the 1-D CNN exhibits the least performance.

4.5 The Robustness Analysis

The Robustness towards different Autoencoder architectures. This section demonstrates the impact of modifications in \mathcal{V} during TGAP on the CG-FedLLM performance, as detailed in Table 4. Our experimental analysis indicates

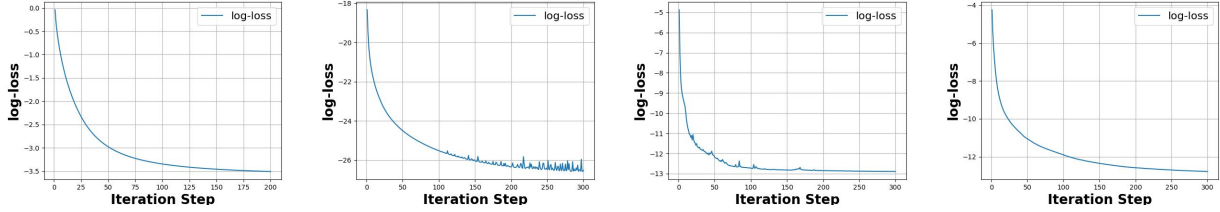


Figure 5: The training curve of the AutoEncoder in TGAP. The leftmost image shows training convergence using 1D-CNN neural networks. The second image depicts training progress with a 0-block U-former neural network. The third image illustrates training convergence with a 1-block U-former neural network, and the rightmost image represents training progress with a 2-block U-former. The x-axis represents the iteration steps, while the y-axis represents the logarithm of the MSE reconstruction loss for AutoEncoder.

Table 3: SNR Analysis for Compression.

	1-D CNN [1]	ResNet [15]	U-Former [47]
$\ [\mathbf{A}, \mathbf{B}]\ _2^2$	14.29	14.29	14.29
$\ [\tilde{\mathbf{A}}, \tilde{\mathbf{B}}] - [\mathbf{A}, \mathbf{B}]\ _2^2$	8.94e-04	5.06e-12	1.04e-11
SNR	1.60e+04	2.82e+12	1.37e+12

that reducing the number of Uformer blocks enhances the performance of fine-tuned models. Achieving zero-block Uformer results in the highest scores across all subjects, except for ‘‘Social Science’’, which is consistent with the zero-block Uformer achieves the smallest log-loss in Auto-Encoder training. Compared to the **Base** scenario, the zero-block Uformer improvements range between 5.6 and 6.9. Relative to the **Cent** scenario, the top score sees an increase of up to 3.8. In comparison with the **LoRA-FT** scenario, improvements reach 2.4 in the category Avg (hard). To conclude, the smaller the number of U-former building blocks, the better the fine-tuned model performance. Furthermore, adjustments were made to the count of the up-sampling and down-sampling blocks within **Enc** and **Dec**, maintaining the number of U-former blocks at 3. It was observed that decreasing the number of upsampling and downsampling blocks to 4 (**Compress-FT-LLaMa-Upsampling-4**) resulted in superior performance of the fine-tuned model compared to completely eliminating the U-former blocks.

Robustness against noise in the gradients, differential privacy situation. To protect differential privacy for the transmitted low-rank matrices, a small amount of Gaussian noise is introduced to the decompositions \mathbf{A} and \mathbf{B} . The AutoEncoder is designed to effectively minimize noise during the compression phase. Various intensities of noise are applied to the transmitted data. Interestingly, adding a small amount of noise before compression improves the effectiveness of fine-tuned LLM models, indicating that a minimal level of noise can enhance the robustness of these models. In contrast, the same level of Gaussian noise is applied to the **LoRA-FT** scenarios without compression for comparison. Assessments indicate that this Gaussian noise negatively impacts model performance. Additionally, an increase in the Gaussian noise magnitude leads to a significant deterioration in the performance of the **LoRA-FT**.

5 Conclusion

In summary, to address the communication efficiency and privacy guarantee issues in federated fine-tuning of LLMs, we propose a novel gradient compression method utilizing pre-trained AutoEncoders. The encoder is kept on the local client, while the decoder is adopted on the server. Through compressed federated fine-tuning, our methods achieve superior performance in representative evaluations. Furthermore, a detailed analysis encompassing the signal-to-noise ratio, compression ratio, and robustness in the noised gradients further verifies the effectiveness of our proposed compression method. One limitation of our work is the additional training and inference cost that the AutoEncoder brings. Although the additional cost is not heavy (e.g., only a few minutes for training in this paper), we will explore more efficient architecture and training strategy in the future.

Table 4: A Comparison of C-Eval with Various Auto-encoder Architecture.

Methods	Stem	Social Sciences	Humanities	Others	Average	Avg(hard)
Compress-FT-LLaMa-Uformer-0	26.8	25.3	26.4	26.6	26.4	27.2
Compress-FT-LLaMa-Uformer-1	26.6	26.5	25.5	25.7	26.2	26.8
Compress-FT-LLaMa-Uformer-2	22.7	23.7	22.8	23.5	23.1	22.7
Compress-FT-LLaMa-Upsampling-4	26.8	25.3	26.4	26.6	26.4	27.3
Compress-FT-LLaMa-Upsampling-2	26.6	26.5	25.5	25.7	26.2	26.8
Compress-FT-LLaMa-Upsampling-1	26.6	26.6	25.6	25.7	26.2	26.8
LoRA-FT-LLaMa	25.9	27.6	25.2	24.5	25.8	24.8

Table 5: A Comparison of C-Eval with Noise in Gradients.

Methods	Stem	Social Sciences	Humanities	Others	Average	Avg(hard)
Noised-Compress-FT-LLaMa $\sigma = 5 \cdot 10^{-1}$	24.8	24.8	24.2	24.5	24.6	25.7
Noised-Compress-FT-LLaMa $\sigma = 5 \cdot 10^{-2}$	24.5	24.9	24.1	24.4	24.5	26.1
Noised-Compress-FT-LLaMa $\sigma = 5 \cdot 10^{-3}$	24.1	26.5	24.0	24.2	24.6	25.3
Noised-Compress-FT-LLaMa $\sigma = 5 \cdot 10^{-4}$	26.8	25.3	26.4	26.6	26.4	27.2
Noised-Compress-FT-LLaMa $\sigma = 5 \cdot 10^{-5}$	26.6	26.0	26.0	25.7	26.3	26.8
Noised-LoRA-FT-LLaMa $\sigma = 5 \cdot 10^{-3}$	21.8	23.3	23.6	23.3	22.8	20.2
Noised-LoRA-FT-LLaMa $\sigma = 5 \cdot 10^{-4}$	23.6	25.1	25.1	24.3	24.4	21.6
Noised-LoRA-FT-LLaMa $\sigma = 5 \cdot 10^{-5}$	24.3	25.6	24	23.6	24.3	24.1
Compress-FT-LLaMa	26.6	26.5	25.5	25.7	26.2	26.8
LoRA-FT-LLaMa	25.9	27.6	25.2	24.5	25.8	24.8

References

- [1] Lusine Abrahamyan, Yiming Chen, Giannis Bekoulis, and Nikos Deligiannis. Learned gradient compression for distributed deep learning. *IEEE Transactions on Neural Networks and Learning Systems*, 33(12):7330–7344, 2021.
- [2] Keith Bonawitz, Vladimir Ivanov, Ben Kreuter, Antonio Marcedone, H Brendan McMahan, Sarvar Patel, Daniel Ramage, Aaron Segal, and Karn Seth. Practical secure aggregation for federated learning on user-held data. *arXiv preprint arXiv:1611.04482*, 2016.
- [3] Somnath Chakrabarti, Thomas Knauth, Dmitrii Kuvaiskii, Michael Steiner, and Mona Vij. Trusted execution environment with intel sgx. In *Responsible Genomic Data Sharing*, pages 161–190. Elsevier, 2020.
- [4] Mingzhe Chen, Nir Shlezinger, H Vincent Poor, Yonina C Eldar, and Shuguang Cui. Communication-efficient federated learning. *Proceedings of the National Academy of Sciences*, 118(17):e2024789118, 2021.
- [5] Mike Conover, Matt Hayes, Ankit Mathur, Jianwei Xie, Jun Wan, Sam Shah, Ali Ghodsi, Patrick Wendell, Matei Zaharia, and Reynold Xin. Free dolly: Introducing the world’s first truly open instruction-tuned llm. *Company Blog of Databricks*, 2023.
- [6] Victor Costan and Srinivas Devadas. Intel sgx explained. *Cryptology ePrint Archive*, 2016.
- [7] Lydia de la Torre. A guide to the california consumer privacy act of 2018. *Available at SSRN 3275571*, 2018.
- [8] Tim Dettmers, Artidoro Pagnoni, Ari Holtzman, and Luke Zettlemoyer. Qlora: Efficient finetuning of quantized llms. *Advances in Neural Information Processing Systems*, 36, 2024.
- [9] Ning Ding, Yujia Qin, Guang Yang, Fuchao Wei, Zonghan Yang, Yusheng Su, Shengding Hu, Yulin Chen, Chi-Min Chan, Weize Chen, et al. Parameter-efficient fine-tuning of large-scale pre-trained language models. *Nature Machine Intelligence*, 5(3):220–235, 2023.
- [10] Zhengxiao Du, Yujie Qian, Xiao Liu, Ming Ding, Jiezhong Qiu, Zhilin Yang, and Jie Tang. GLM: General language model pretraining with autoregressive blank infilling. In *Proceedings of the 60th Annual Meeting of the Association for Computational Linguistics (Volume 1: Long Papers)*, pages 320–335, 2022.
- [11] Zhengxiao Du, Yujie Qian, Xiao Liu, Ming Ding, Jiezhong Qiu, Zhilin Yang, and Jie Tang. GLM: general language model pretraining with autoregressive blank infilling. pages 320–335, 2022.

- [12] Haokun Fang and Quan Qian. Privacy preserving machine learning with homomorphic encryption and federated learning. *Future Internet*, 13(4):94, 2021.
- [13] Zihao Fu, Haoran Yang, Anthony Man-Cho So, Wai Lam, Lidong Bing, and Nigel Collier. On the effectiveness of parameter-efficient fine-tuning. In *Proceedings of the AAAI Conference on Artificial Intelligence*, volume 37, pages 12799–12807, 2023.
- [14] Jonas Geiping, Hartmut Bauermeister, Hannah Dröge, and Michael Moeller. Inverting gradients-how easy is it to break privacy in federated learning? *Advances in Neural Information Processing Systems*, 33:16937–16947, 2020.
- [15] Kaiming He, Xiangyu Zhang, Shaoqing Ren, and Jian Sun. Deep residual learning for image recognition. In *Proceedings of the IEEE conference on computer vision and pattern recognition*, pages 770–778, 2016.
- [16] Dan Hendrycks, Collin Burns, Steven Basart, Andy Zou, Mantas Mazeika, Dawn Song, and Jacob Steinhardt. Measuring massive multitask language understanding. *arXiv preprint arXiv:2009.03300*, 2020.
- [17] Neil Houlsby, Andrei Giurgiu, Stanislaw Jastrzebski, Bruna Morrone, Quentin De Laroussilhe, Andrea Gesmundo, Mona Attariyan, and Sylvain Gelly. Parameter-efficient transfer learning for nlp. In *International conference on machine learning*, pages 2790–2799. PMLR, 2019.
- [18] Edward J Hu, Yelong Shen, Phillip Wallis, Zeyuan Allen-Zhu, Yuanzhi Li, Shean Wang, Lu Wang, and Weizhu Chen. Lora: Low-rank adaptation of large language models. *arXiv preprint arXiv:2106.09685*, 2021.
- [19] Yuzhen Huang, Yuzhuo Bai, Zhihao Zhu, Junlei Zhang, Jinghan Zhang, Tangjun Su, Junteng Liu, Chuancheng Lv, Yikai Zhang, Yao Fu, et al. C-eval: A multi-level multi-discipline chinese evaluation suite for foundation models. *Advances in Neural Information Processing Systems*, 36, 2024.
- [20] Shima Imani, Liang Du, and Harsh Shrivastava. Mathprompter: Mathematical reasoning using large language models. *arXiv preprint arXiv:2303.05398*, 2023.
- [21] Don H Johnson. Signal-to-noise ratio. *Scholarpedia*, 1(12):2088, 2006.
- [22] Nikitas Karanikolas, Eirini Manga, Nikoleta Samaridi, Eleni Tousidou, and Michael Vassilakopoulos. Large language models versus natural language understanding and generation. In *Proceedings of the 27th Pan-Hellenic Conference on Progress in Computing and Informatics*, pages 278–290, 2023.
- [23] Jakub Konečný, H Brendan McMahan, Felix X Yu, Peter Richtárik, Ananda Theertha Suresh, and Dave Bacon. Federated learning: Strategies for improving communication efficiency. *arXiv preprint arXiv:1610.05492*, 8, 2016.
- [24] Li Li, Yuxi Fan, Mike Tse, and Kuo-Yi Lin. A review of applications in federated learning. *Computers & Industrial Engineering*, 149:106854, 2020.
- [25] Haokun Liu, Derek Tam, Mohammed Muqeeth, Jay Mohta, Tenghao Huang, Mohit Bansal, and Colin A Raffel. Few-shot parameter-efficient fine-tuning is better and cheaper than in-context learning. *Advances in Neural Information Processing Systems*, 35:1950–1965, 2022.
- [26] Shih-Yang Liu, Chien-Yi Wang, Hongxu Yin, Pavlo Molchanov, Yu-Chiang Frank Wang, Kwang-Ting Cheng, and Min-Hung Chen. Dora: Weight-decomposed low-rank adaptation. *arXiv preprint arXiv:2402.09353*, 2024.
- [27] Brady D Lund and Ting Wang. Chatting about chatgpt: how may ai and gpt impact academia and libraries? *Library hi tech news*, 40(3):26–29, 2023.
- [28] Priyanka Mary Mammen. Federated learning: Opportunities and challenges. *arXiv preprint arXiv:2101.05428*, 2021.
- [29] Mohamad Mansouri, Melek Önen, Wafa Ben Jaballah, and Mauro Conti. Sok: Secure aggregation based on cryptographic schemes for federated learning. *Proceedings on Privacy Enhancing Technologies*, 2023.
- [30] Brendan McMahan, Eider Moore, Daniel Ramage, Seth Hampson, and Blaise Aguerre y Arcas. Communication-efficient learning of deep networks from decentralized data. In *Artificial intelligence and statistics*, pages 1273–1282. PMLR, 2017.
- [31] Viraaji Mothukuri, Reza M Parizi, Seyedamin Pouriyeh, Yan Huang, Ali Dehghantanha, and Gautam Srivastava. A survey on security and privacy of federated learning. *Future Generation Computer Systems*, 115:619–640, 2021.
- [32] Amirhossein Reisizadeh, Aryan Mokhtari, Hamed Hassani, Ali Jadbabaie, and Ramtin Pedarsani. Fedpaq: A communication-efficient federated learning method with periodic averaging and quantization. In *International conference on artificial intelligence and statistics*, pages 2021–2031. PMLR, 2020.
- [33] Nir Shlezinger, Mingzhe Chen, Yonina C Eldar, H Vincent Poor, and Shuguang Cui. Uveqfed: Universal vector quantization for federated learning. *IEEE Transactions on Signal Processing*, 69:500–514, 2020.

- [34] Jiaxing Sun, Weiquan Huang, Jiang Wu, Chenya Gu, Wei Li, Songyang Zhang, Hang Yan, and Conghui He. Benchmarking chinese commonsense reasoning of llms: From chinese-specifics to reasoning-memorization correlations. *arXiv preprint arXiv:2403.14112*, 2024.
- [35] Zhiwei Tang, Yanmeng Wang, and Tsung-Hui Chang. z-signfedavg: A unified stochastic sign-based compression for federated learning. In *Proceedings of the AAAI Conference on Artificial Intelligence*, volume 38, pages 15301–15309, 2024.
- [36] Rohan Taori, Ishaan Gulrajani, Tianyi Zhang, Yann Dubois, Xuechen Li, Carlos Guestrin, Percy Liang, and Tatsunori B. Hashimoto. Stanford alpaca: An instruction-following llama model. https://github.com/tatsu-lab/stanford_alpaca, 2023.
- [37] Sasha Targ, Diogo Almeida, and Kevin Lyman. Resnet in resnet: Generalizing residual architectures. *arXiv preprint arXiv:1603.08029*, 2016.
- [38] Hugo Touvron, Thibaut Lavril, Gautier Izacard, Xavier Martinet, Marie-Anne Lachaux, Timothée Lacroix, Baptiste Rozière, Naman Goyal, Eric Hambro, Faisal Azhar, et al. Llama: Open and efficient foundation language models. *arXiv preprint arXiv:2302.13971*, 2023.
- [39] Stacey Truex, Nathalie Baracaldo, Ali Anwar, Thomas Steinke, Heiko Ludwig, Rui Zhang, and Yi Zhou. A hybrid approach to privacy-preserving federated learning. In *Proceedings of the 12th ACM workshop on artificial intelligence and security*, pages 1–11, 2019.
- [40] Stacey Truex, Ling Liu, Ka-Ho Chow, Mehmet Emre GURSOY, and Wenqi Wei. Ldp-fed: Federated learning with local differential privacy. In *Proceedings of the third ACM international workshop on edge systems, analytics and networking*, pages 61–66, 2020.
- [41] Dmitry Ulyanov, Andrea Vedaldi, and Victor Lempitsky. Deep image prior. In *Proceedings of the IEEE conference on computer vision and pattern recognition*, pages 9446–9454, 2018.
- [42] Ashish Vaswani, Noam Shazeer, Niki Parmar, Jakob Uszkoreit, Llion Jones, Aidan N Gomez, Łukasz Kaiser, and Illia Polosukhin. Attention is all you need. *Advances in neural information processing systems*, 30, 2017.
- [43] Paul Voigt and Axel Von dem Bussche. The eu general data protection regulation (gdpr). *A Practical Guide, 1st Ed., Cham: Springer International Publishing*, 10(3152676):10–5555, 2017.
- [44] Jialei Wang, Mladen Kolar, Nathan Srebro, and Tong Zhang. Efficient distributed learning with sparsity. In *International conference on machine learning*, pages 3636–3645. PMLR, 2017.
- [45] Siyuan Wang, Zhongyu Wei, Yejin Choi, and Xiang Ren. Can llms reason with rules? logic scaffolding for stress-testing and improving llms. *arXiv preprint arXiv:2402.11442*, 2024.
- [46] Yansheng Wang, Yongxin Tong, and Dingyuan Shi. Federated latent dirichlet allocation: A local differential privacy based framework. In *Proceedings of the AAAI Conference on Artificial Intelligence*, volume 34, pages 6283–6290, 2020.
- [47] Zhendong Wang, Xiaodong Cun, Jianmin Bao, Wengang Zhou, Jianzhuang Liu, and Houqiang Li. Uformer: A general u-shaped transformer for image restoration. In *Proceedings of the IEEE/CVF conference on computer vision and pattern recognition*, pages 17683–17693, 2022.
- [48] Jianqiao Wangni, Jialei Wang, Ji Liu, and Tong Zhang. Gradient sparsification for communication-efficient distributed optimization. *Advances in Neural Information Processing Systems*, 31, 2018.
- [49] Kang Wei, Jun Li, Ming Ding, Chuan Ma, Howard H Yang, Farhad Farokhi, Shi Jin, Tony QS Quek, and H Vincent Poor. Federated learning with differential privacy: Algorithms and performance analysis. *IEEE transactions on information forensics and security*, 15:3454–3469, 2020.
- [50] Zhengxuan Wu, Aryaman Arora, Zheng Wang, Atticus Geiger, Dan Jurafsky, Christopher D Manning, and Christopher Potts. Reft: Representation finetuning for language models. *arXiv preprint arXiv:2404.03592*, 2024.
- [51] Jie Xu, Benjamin S Glicksberg, Chang Su, Peter Walker, Jiang Bian, and Fei Wang. Federated learning for healthcare informatics. *Journal of healthcare informatics research*, 5:1–19, 2021.
- [52] Aohan Zeng, Xiao Liu, Zhengxiao Du, Zihan Wang, Hanyu Lai, Ming Ding, Zhuoyi Yang, Yifan Xu, Wendi Zheng, Xiao Xia, et al. Glm-130b: An open bilingual pre-trained model. *arXiv preprint arXiv:2210.02414*, 2022.
- [53] Chengliang Zhang, Suyi Li, Junzhe Xia, Wei Wang, Feng Yan, and Yang Liu. {BatchCrypt}: Efficient homomorphic encryption for {Cross-Silo} federated learning. In *2020 USENIX annual technical conference (USENIX ATC 20)*, pages 493–506, 2020.
- [54] Jianshi Zhang, Martin Kuo, Ruiyi Zhang, Guoyin Wang, Saeed Vahidian, and Yiran Chen. Shepherd: A lightweight github platform supporting federated instruction tuning. <https://github.com/JayZhang42/FederatedGPT-Shepherd>, 2023.

- [55] Jianyi Zhang, Saeed Vahidian, Martin Kuo, Chunyuan Li, Ruiyi Zhang, Guoyin Wang, and Yiran Chen. Towards building the federated gpt: Federated instruction tuning, 2023.
- [56] Ligeng Zhu, Zhijian Liu, and Song Han. Deep leakage from gradients. In H. Wallach, H. Larochelle, A. Beygelzimer, F. d'Alché-Buc, E. Fox, and R. Garnett, editors, *Advances in Neural Information Processing Systems*, volume 32. Curran Associates, Inc., 2019.